Spiral wave stability in cardiac tissue with biphasic restitution

O. Bernus and H. Verschelde
Department of Mathematical Physics and Astronomy, Ghent University, Krijgslaan 281, 9000 Gent, Belgium

A. V. Panfilov
Department of Theoretical Biology, Utrecht University, Padualaan 8, 3584 CH Utrecht, The Netherlands

(Received 4 November 2002; revised manuscript received 25 April 2003; published 26 August 2003)

Human ventricular tissue as well as several animal ventricular preparations show a biphasic shape of the action potential duration restitution curve, with a local maximum at low diastolic intervals. We study numerically how the location and properties of this nonmonotonicity affect the stability of spiral waves. We find that, depending on the slopes of the ascending and of the descending parts of the restitution curve, we can have either stable rotation of the spiral wave or spiral breakup. We identify two types of spiral breakup: one due to a steep positive slope and another due to a steep negative slope in the restitution curve. We discuss the differences in their manifestation and possible implications. We also find that increasing the slope of the descending part of the restitution curve increases the meandering of the spiral wave, due to the repeated occurrence of conduction blocks near the spiral wave tip.

DOI: 10.1103/PhysRevE.68.021917 PACS number(s): 87.10.+e, 82.40.Ck, 87.19.Hh

I. INTRODUCTION

Many cardiac arrhythmias are characterized by rotating waves of excitation [1,2], which are similar to spiral waves found in a wide variety of nonlinear excitable media [3]. The dynamics of spiral waves are considered to play a determining role in the type of cardiac arrhythmia. In general, stationary rotation of spiral waves is associated with stationary arrhythmias with a periodic ECG (monomorphic tachycardia), while unstable rotation of spiral wave (meandering [4]), and especially spiral breakup, which is a deterioration of a single spiral wave into a spatiotemporal chaos, is associated with more complex arrhythmias and cardiac fibrillation, which is the leading cause of death in the industrialized world (see Ref. [5] for details).

It has been shown that the onset of the spiral breakup in some cases can heavily depend on a cellular property called ''restitution of action potential duration,'' which is a dependency of the duration of cardiac action potential $[t(\mathrm{APD})]$ on the time since the end of a preceding action potential, called diastolic interval $[t(\mathrm{DI})]$. Normally, a longer $t(\mathrm{DI})$ yields a longer $t(\mathrm{APD})$, so that the restitution curve is a monotonically increasing function of $t(\mathrm{DI})$ [6,7]. An important characteristic of the restitution curve is its maximal slope at low $t(\mathrm{DI})$. It has been shown that spiral waves can break up and develop a fibrillationlike pattern when the absolute value of the slope of the restitution curve exceeds unity. This has been confirmed in numerous simulations of excitable media [8–12].

Some experimental studies have however reported the existence of restitution curves with a different shape. Experimental measurements of $t(\mathrm{APD})$ restitution in human ventricular tissue revealed that it can have a nonmonotonic (biphasic) shape, with a local maximum and a local minimum at low diastolic intervals [Figs. 1(a)–1(d)] [13,14]. Similar restitution curves were reported in rabbit [15] as well as in some dog preparations [16,17]. The influence of biphasic restitution on reentrant arrhythmias has been investigated in experimental and numerical studies of one-dimensional (1D) maps [18] and for circulating pulse in a 1D ring of tissue [19]. The general conclusion of these studies was that biphasic restitution can increase the complexity of the dynamics of the arrhythmia. However, the influence of biphasic restitution on spiral waves in two- (or more) dimensional media was not investigated. Zemlin and Panfilov [20] showed that a negative slope in the restitution curve, which is a characteristic feature of biphasic restitution, can substantially affect the spiral wave dynamics and can cause spiral breakup when it becomes steeper than -1. They, however, only considered the case of monotonically decreasing restitution curves, which do not have a local maximum at low $t(\mathrm{DI})$. Recently, Fenton *et al.* demonstrated breakup of spiral waves in an excitable medium with biphasic restitution curve [21]. However, the above mentioned studies were done for a single shape of the $t(\mathrm{APD})$ restitution curve, which was not fit to experimentally measured curves in human ventricular tissue. Moreover, no detailed analysis was performed of the size and location of the biphasic restitution properties on spiral wave dynamics.

The main aim of the present work is to study the effect of biphasic restitution on spiral wave dynamics in a model that fits experimentally measured restitution curves of human ventricular tissue and reproduces basic properties of human cardiac action potential [22]. We study the properties of spiral wave under variations of the most important characteristics of the biphasic restitution curve: the amplitude of the nonmonotonic part, the magnitude of the positive slope at low $t(\mathrm{DI})$, and the magnitude of the negative slope at intermediate $t(\mathrm{DI})$.

II. MODEL

Ionic models of cardiac tissue are described by the following equation:

$$C_m \partial_t V_m = d\nabla^2 V_m - I_{ion}, \tag{1}$$

where V_m is the membrane potential, C_m is the membrane capacitance, d is a diffusion matrix, and I_{ion} is the sum of the transmembrane currents as described in Ref. [22], where g_K and g_{K1} have been increased to 0.033 nS/pF, and 5.5 nS/pF, respectively, to yield t(APD) in the range reported by Ref. [6].

The precise mechanism underlying biphasic restitution is still poorly understood, but it was suggested to be the result of a supernormal behavior of the calcium dynamics resulting in increased calcium channel activity [6,23]. Hence, we reproduced biphasic restitution in a phenomenological way, by modification of the L-type calcium channel in ionic models. The equation of the L-type calcium current I_{Ca} in the original model is given by

$$I_{\mathrm{Ca}}=g_{\mathrm{Ca}}df(V_m-E_{\mathrm{Ca}}), \tag{2}$$

where g_{Ca} denotes the conductance, E_{Na} is the reversal potential, and d and f are gating variables of the Hodgkin-Huxley-type [24], fulfilling a relaxation equation of the same type as Eq. (4).

It is known that t(APD) is correlated to the amplitude of I_{Ca}, larger amplitude results in longer t(APD). In order to reproduce biphasic restitution we replaced the constant value g_{Ca} by $g_{Ca}+g_{Ca}S(c(\mathrm{DI}))$, where $S(c(\mathrm{DI}))$ is a function of c(DI) [computed t(DI), see explanation later in the text]. $S(c(\mathrm{DI}))$ is zero for almost all values of the argument, and is positive in a small interval of c(DI), corresponding to the bump of the biphasic restitution curve. Basically, this function generates an extra inward current, which elongates t(APD) for short t(DI). Using the following sigmoidal functions, we are able to design the function $S(c(\mathrm{DI}))$ in a controllable way:

$$S(c(\mathrm{DI}))=A\{1-\tanh[a_-(c(\mathrm{DI})-d_-)]\}\times\{1+\tanh[a_+(c(\mathrm{DI})-d_+)]\}. \tag{3}$$

By changing the parameters A, a_+, a_-, d_+, and d_- we can fit the shape and location of the biphasic bump to any experimentally obtained curve.

In order to make our fits as close as possible to real experimental data, we need to correlate c(DI) to the real diastolic interval. However, the real t(DI) is not a variable of ionic models. Moreover, its calculation should be autonomous and not obtained from previous activation times as in Ref. [19], in order to be valid in 2D. Therefore, we introduced a new gating variable d_s with the following dynamics:

$$\partial_t d_s=\frac{d_{s,\infty}(V_m)-d_s}{\tau_{d_s}(V_m)} \tag{4}$$

with

$$d_{s,\infty}=5.0,\quad \tau_{d_s}=10.0\quad \text{for}\ \ V_m\in[-55,-40] \tag{5}$$

$$d_{s,\infty}=1.0,\quad \tau_{d_s}=200.0\quad \text{for}\ \ V_m<-55 \tag{6}$$

$$d_{s,\infty}=1.0,\quad \tau_{d_s}=5000.0\quad \text{for}\ V_m>-40. \tag{7}$$

TABLE I. Different parameter sets for the biphasic restitution curves.

	Set 1	Set 2	Set 3	Set 4
d_-	125	125	100	95
d_+	35	−25	10	30
a_+	0.025	0.025	0.125	0.175
a_-	0.04	0.016	0.016	0.016

It is easy to see that at the back of the ''preceding action potential,'' when V_m decreases from −40 to −55 the value of d_s becomes close to 5.0, and then (until the next pulse) exponentially decays to the value 1.0 with a time constant of 200.0 ms. The time constant of 5000.0 ms when $V_m>-40$ guarantees that d_s remains almost unchanged over the bulk of the action potential (till its back). It can then be found that t(DI) can be evaluated from the value of d_s by the following equation:

$$c(\mathrm{DI})=-20-200\ln\frac{d_s-1}{4}. \tag{8}$$

Equations (3), (4), and (8) provide a framework for fitting basic restitution curves of human ventricular tissue and make desired modifications thereof. Note that the several constants used for such a fitting, for example, $d_{s,\infty}=5.0, \tau_{d_s}=5000.0$, are phenomenological and one can easily achieve similar fits using other numerical values.

In this paper, we used four different sets of parameter values (d_-,d_+,a_-,a_+) in order to obtain different biphasic restitution curves (Table I, $A=0.32$ in all cases). Set 1 reproduces the experimental curve of Morgan *et al.* [14], with a steep positive slope at low t(DI) and $dt(\mathrm{APD})/dt(\mathrm{DI})>-1$ everywhere [Fig. 1(a)]. Using set 2 we obtained the same curve as in the case of set 1, except for the positive slope at low t(DI), the steepness of which was reduced below 1 [Fig. 1(b)]. For parameter sets 3 and 4 the steepness of the negative slope region of parameter set 2 was increased, with a region of $dt(\mathrm{APD})/dt(\mathrm{DI})<-1$ in both cases [Figs. 1(c) and 1(d)]. The restitution curves were calculated by means of an $S1$-$S2$ protocol in a single cell, consisting of 10 $S1$ stimuli at 1 Hz frequency and an extra stimulus at some t(DI) after the last $S1$ AP, and plotting its t(APD) at 90% repolarization versus t(DI).

We used the operator-splitting method to split Eq. (1) into an ordinary differential equation (ODE) for reaction (I_{ion}) and a partial differential equation (PDE) for diffusion. The PDE was solved using an alternating-direction implicit scheme [25] at a spatial discretisation of $\Delta x=0.025$ cm (isotropic medium with 1500×1500 cells), whereas for the ODE we used a time-adaptive forward Euler scheme with two possible time steps, $\Delta t_{min}=0.02$ ms and $\Delta t_{max}=0.1$ ms. In this scheme, for each point of the medium the ODE is solved with Δt_{max}; if $dV_m/dt<1$ V/s we move on to the next point, otherwise we integrate the ODE at that point five times with Δt_{min} from its initial value. The relaxation equations for the gating variables were integrated using a technique pre-

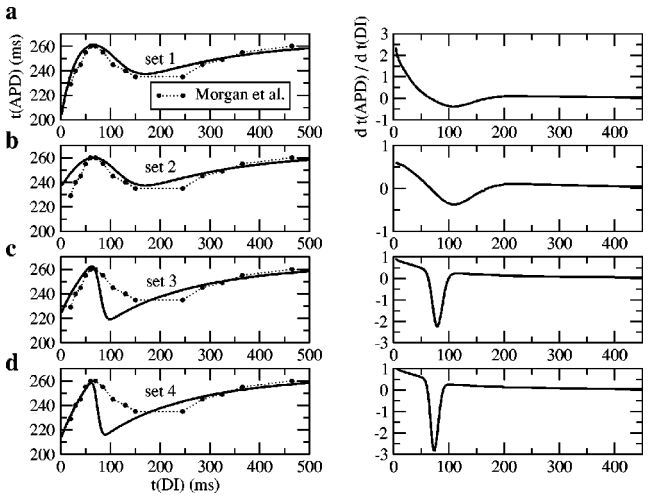

FIG. 1. Restitution curves (left) and their slopes (right) for the different parameter sets compared to experimental data obtained by Morgan *et al.* [6]: (a) set 1, (b) set 2, (c) set 3, and (d) set 4.

sented by Rush and Larsen [26]. We used the no-flux boundary condition. All simulations were coded in C^{++} and run either on a Dell 530 Precision Workstation with two Intel Xeon 2.0 GHz processors.

We obtained spiral waves using an $S1$-$S2$ protocol. We first paced one side of the tissue ($S1$) producing a plane wave propagating in one direction. When the refractory tail of this wave crossed the middle of the medium, we moved our pacing electrode to that site and applied a single stimulus ($S2$) parallel to the $S1$ wave front but not over the whole width of the medium. Stimulus currents lasted for 2 ms ($S1$) and 5 ms ($S2$) and their strength was two times the threshold for both. The $S2$ wave front curled around its free end and produced a spiral wave. The position of the spiral tip was calculated using an algorithm presented by Fenton and Karma [27].

III. RESULTS

A. From monotonic to biphasic restitution

Although the restitution curve, which is the best fit for the experimental data obtained by Morgan *et al.* [14], has a clear biphasic shape (set 1), we started our study from the well known monotonic restitution curve [Fig. 2(a), solid line] and gradually increased the amplitude of the nonmonotonic part by increasing parameter A in Eq. (3), until we obtained the

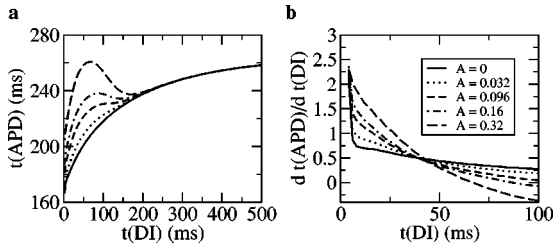

FIG. 2. Restitution curves (left) and their slopes (right) for parameter set 1 where A was varied between 0 and 0.32.

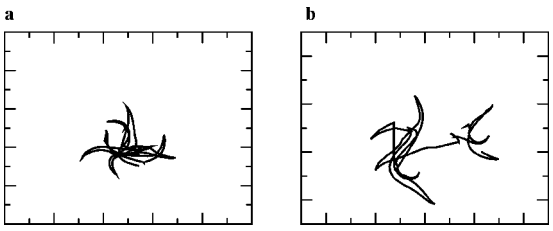

FIG. 3. Trajectory of the spiral wave tips in the case of (a) $A=0.032$ and (b) $A=0.096$ during the interval [1000 ms, 2000 ms]. The graphs have dimensions 12.5 cm×12.5 cm.

biphasic restitution curve that fits the data by Morgan *et al.* [14] (set 1). We studied the dynamics of spiral waves during this process.

For the monotonic restitution curve ($A=0$), where the slope of the restitution curve was larger than 1 in a very small interval [$t(\mathrm{DI})<5$ ms, Fig. 2], we observed a stable meandering behavior of the spiral wave, with a linear core of 4.6 cm and a rotational period of about 220 ms, which was similar to the results of our previous study [22] adjusted for the shortened action potential. When the amplitude of the nonmonotonic part increased, we found increasingly more complex meandering patterns with multiple areas of conduction block forming close to the spiral tip. These blocks were, however, never effective in creating new spiral waves by the breakup process, but merely affected the trajectory of the spiral tip. This effect is illustrated in Fig. 3, and is further discussed in the following section.

When A became larger than 0.16, the region of the restitution curve with $dt(\mathrm{APD})/dt(\mathrm{DI})>1$ was large enough to destabilize the spiral wave and to cause breakup after a few rotations. Hence, we found that for the best fit of the experimental data ($A=0.32$) spiral waves are unstable and break down in multiple daughter wavelets after the fourth rotation. From then on a complex activation pattern sets in, where new spiral waves are formed via the breakup process and other disappears at boundaries or when coalescing (Fig. 4).

Thus, we observed two main effects: (1) when the amplitude of the nonmonotonicity increased, the meandering of the spiral wave became more pronounced, (2) when the positive slope of the left branch of the restitution curve became steeper than 1 over a large interval, breakup occurred. In order to study these processes separately, we fixed the amplitude of the nonmonotonic part as in set 1 ($A=0.32$) and varied the slopes of the regions with positive and negative restitution.

FIG. 4. Spiral breakup using parameter set 1. Snapshots of electrical activity going from left to right. Activity is displayed in gray shadings going from black (rest) to white (fully activated). The first frame was taken at 1.9 s and the frames are separated by time steps of 50 ms. The frames have dimensions 37.5 cm×37.5 cm.

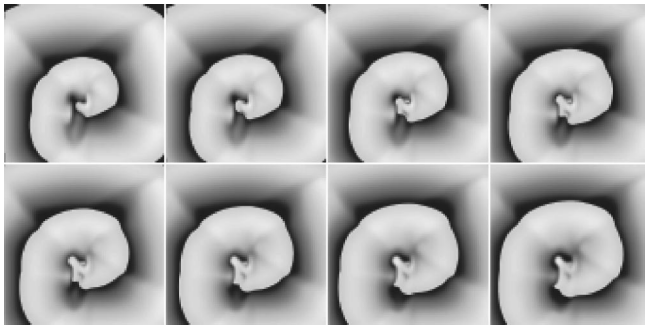

FIG. 5. Conduction block near the spiral tip in the case of parameter set 3. Snapshots of electrical activity going from left to right and from top to bottom. Activity is displayed in gray shadings going from black (rest) to white (fully activated). The first frame was taken at 1.25 s model time and the frames are separated by time steps of 10 ms. The frames have dimensions 37.5 cm×37.5 cm.

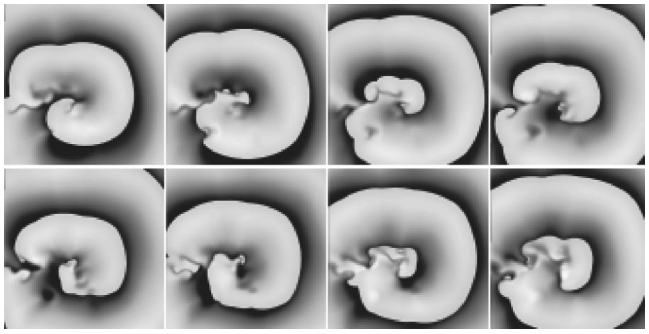

FIG. 6. Spiral breakup using parameter set 3. Snapshots of electrical activity going from left to right and from top to bottom. Activity is displayed in gray shadings going from black (rest) to white (fully activated). The first frame was taken at 7.9 s model time and the frames are separated by time steps of 50 ms. The frames have dimensions 37.5 cm×37.5 cm.

B. Effects of the ascending and descending parts of the restitution curve on spiral wave dynamics

It is reasonable to assume that in the case of parameter set 1 breakup is due to a steep restitution curve, as the slope of the restitution curve exceeds unity at short diastolic intervals [Fig. 1(a), right]. This type of unstable behavior resulting in breakup of the wave front corresponds to spiral wave breakup observed in models of monotonic increasing restitution curves with a steep slope [11,28,29].

In order to check this hypothesis we have studied a spiral wave in the case of set 2, where the magnitude of the positive slope at low $t(\mathrm{DI})$ was reduced below 1 [Fig. 1(b)]. We found that in this case the spiral wave remained stably rotating without any breakup. The period of spiral wave was about 230 ms and it had a $t(\mathrm{DI})$ of 22 ms. The core was linear and had a diameter of about 5 cm [Fig. 7(a)]. The wavelength (the product of the period and conduction velocity) was ≈ 11.5 cm.

Note that, for both sets 1 and 2 the slope of the negatively sloped part of the restitution curve was never lower than the critical value -1, for which one could expect the onset of instabilities [20]. Therefore we used parameter set 3 which has a minimal negative slope of about -2, while the maximal positive slope is below 1. We found that in this case the rotation of spiral became more instable. We repeatedly observed areas of conduction block forming close to the spiral tip and obtained, as a result, a complex meandering pattern that consisted of two processes: rotation along a linear core, which in this case is about 50% longer than for set 2, and a drift of the spiral over a substantial distance (due to the conduction block) [Figs. 5, 7(a,b)]. This was similar to the processes observed in the preceding section, which were responsible for the increased complexity of the meandering pattern in Fig. 3. Ineffective breaks of spiral formed in the spiral arm starting from approximately fifth rotation, but these were not successful in creating new spiral waves, and a single spiral wave persisted for as long as 8.3 s (or about 30 rotations). It rotated with an average period of 230 ms (the same as for set 2) but the $t(\mathrm{DI})$ was increased to the value of about 35 ms. At 8.3 s we observed an effective breakup and afterwards a complex activation pattern set in, as illustrated by Fig. 6.

In order to study the role of the magnitude of the negative slope in the dynamics of the spiral wave, we used parameter set 4 where the steepness of the negative restitution was further increased [Fig. 1(d)]. We found an increased instable behavior of the spiral wave: tip motion became more complex and the spiral wave showed a substantial drift in space [Fig. 7(c)]. However, effective breakup here required a longer time and occurred around 10 s. Afterwards, a complex pattern similar to that of Fig. 6 was formed. We also found that the average $t(\mathrm{DI})$ of the spiral wave was further increased to 50 ms. This seems to be correlated with observations made by Zemlin and Panfilov [20], who showed that spiral waves with more negative slope have longer $t(\mathrm{DI})$. In our case, as in Ref. [20], the increase of $t(\mathrm{DI})$ was achieved by a larger tip motion.

In order to check whether the tip motion is important for the deterioration into a complex pattern, we initiated a spiral wave circulating around an unexcitable circular hole for parameter set 3. We chose the radius of the hole to be 2.5 cm in order to have a spiral wave rotating with a $t(\mathrm{DI})=37$ ms, comparable to the unbroken spiral wave in previous simula-

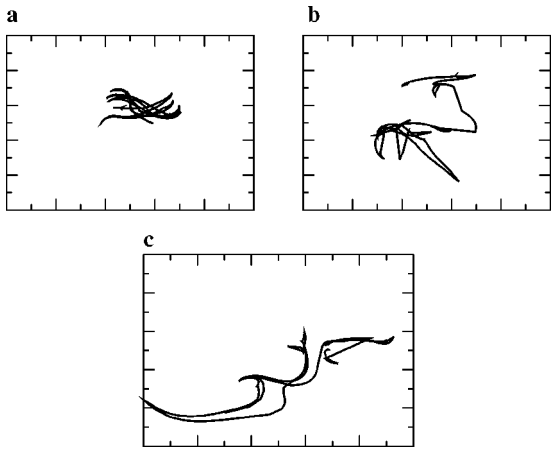

FIG. 7. Trajectory of the spiral wave tips in the case of parameter sets 2 (a), 3 (b), and 4 (c) during the interval [1000 ms, 2000 ms]. The graphs have dimensions 12.5 cm×12.5 cm.

tion with the same parameter set. We found that the reentrant wave remained stable and rotated at a constant $t(\mathrm{DI})$ of 37 ms.

IV. DISCUSSION

The magnitude of the biphasic part of the restitution curve seems to play a role in the stability of the spiral waves. We found that for low magnitudes, with $|dt(\mathrm{APD})/dt(\mathrm{DI})|<1$ everywhere, stable spiral waves can be obtained with a regular meandering pattern. If the amplitude of the biphasic ''bump'' is increased, we first observe a disturbance in the trajectory of the tip, due to conduction blocks created along the spiral arm. We did not observe successful breakups of the spiral wave until the average $t(\mathrm{DI})$ of the spiral wave lied within the unstable region of the restitution curve where the slope was larger than 1. Fenton *et al.* [21] showed that spiral breakup due to biphasic restitution curves with $|dt(\mathrm{APD})/dt(\mathrm{DI})|<1$ could be obtained due to conduction blocks forming along the spiral arm. In our case, we also observed the conduction blocks, but they were never successful in creating new spiral waves, when $|dt(\mathrm{APD})/dt(\mathrm{DI})|<1$. These differences can be explained by two observations: (1) in our simulations the $t(\mathrm{APD})$ is much longer, the saturated value of $t(\mathrm{APD})$ at long $t(\mathrm{DI})$ is about 270 ms, while in Ref. [21] $t(\mathrm{APD})(\infty)\sim 70$ ms, making waves less prone to break up, (2) in Ref. [21] the amplitude of the biphasic bump is about three times larger than the amplitudes discussed in this paper. Hence, the effects of the biphasic part might have been relatively more pronounced in Ref. [21] than in our computations.

We found two types of spiral breakup in a model of human ventricular tissue with biphasic $t(\mathrm{APD})$ restitution. The first type corresponds to previously studied breakup, where the positive slope of the restitution curve exceeds unity at low $t(\mathrm{DI})$ [11]. The second type of breakup was observed when the negative slope became less than -1. In that case the breakup took a longer time to develop (up to 30 spiral wave rotations compared to 4 for the first type), which is similar to the results obtained by Zemlin and Panfilov [20]. We found that this second type of breakup was mainly due to a substantial perturbation of the motion of the tip, when the steepness of the negatively sloped part of the restitution curve gets below -1. This irregular motion enhanced irregularities along the spiral arm via the Doppler effect and eventually caused the wave breaks, similar to the results obtained by Qu *et al.* [30] and Fenton *et al.* [21] in models with monotonous restitution curves. The role of the tip motion was further confirmed by the lack of spiral breakup when a spiral wave was pinned around an unexcitable circular hole in the case of parameter set 3.

We modeled biphasic restitution curves by modifying the calcium current, based on some experimental studies [6,23]. However, until today, there is no agreement on the exact mechanism of biphasic restitution. Our approach can easily be extended to reproduce other mechanisms of nonmonotonicity, for example, by modifying the potassium current conductance g_{K} into $g_{\mathrm{K}}[1-D(c(\mathrm{DI}))]$, with a function $D(c(\mathrm{DI}))$ similar to $S(c(\mathrm{DI}))$ from Eq. (3). Note, that both mechanisms of breakup, which we find in our simulations, were confirmed in a wide variety of computations involving totally different descriptions of cardiac tissue. Therefore we believe that our results reflect basic properties of spiral waves in cardiac tissue with biphasic restitution and should hold independently of the method used to reproduce this nonmonotonic restitution.

The restitution curves were calculated using an $S1$-$S2$ protocol in single ventricular model cells. In experiments [6,14], however, restitution curves are measured in tissue, where electrotonic effects can affect the shape of the restitution curve with respect to the maximal and minimal values of $t(\mathrm{APD})$. We have, for the case of parameter set 2, calculated the restitution curve in a point of a 2D sheet of ventricular cells by simulating unidirectional propagating action potentials at decreasing basic cycle length. The resulting restitution curve showed an overall decrease of $t(\mathrm{APD})$ by an amount of about 15 ms when compared to the curve obtained in a single cell. The slope of the curve was, however, similar in all points ($<5\%$ deviation). Since our study focuses on the effects of the slope of biphasic restitution curves and the amplitude of the bump, we believe that our restitution curves are representative for the observed dynamics in two-dimensional media.

The main limitation of our two-dimensional simulations is that they were based on a homogeneous isotropic medium, whereas the heart is an heterogeneous three-dimensional object with anisotropic properties. Heterogeneities and anisotropy can affect the spiral wave dynamics [31,32], and further studies in more realistic models are therefore required.

Another limitation is the fact that in our case biphasic restitution curves are obtained using an $S1$-$S2$ protocol at a given basic cycle length and that the steady-state restitution curves also have the biphasic ''bump'' (not shown). Biphasic restitution has, however, never been observed during steady-state $t(\mathrm{APD})$ restitution, where each point of the restitution curve is obtained when a steady state is reached for a given basic cycle length [33]. Hence, destabilizing effects of biphasic restitution may be more important only during the first beats of a rapid change of cycle length and less important after several beats because of the cycle length adaptation and the nonbiphasic steady state.

V. CONCLUSION

In conclusion, we found in tissue with biphasic restitution curve two types of spiral breakup: one due to a steep positive slope (>1) and another due to a steep negative (<-1) slope in the restitution curve. We also found that increasing the slope of the descending part or the amplitude of the biphasic part of the restitution curve increases the meandering of the spiral wave, due to the repeated occurrence of conduction blocks near the spiral wave tip.

ACKNOWLEDGMENT

This research was supported by a specialization grant from the Flemish Institute for the Promotion of Scientific and Technological Research in Industry (IWT).

[1] M. Allessie, F. Bonke, and F. Schopman, Circ. Res. **33**, 54 (1973).
[2] J. Davidenko, A. Pertsov, R. Salomontsz, W. Baxter, and J. Jalife, Nature (London) **355**, 349 (1991).
[3] A. Winfree and S. Strogatz, Nature (London) **311**, 611 (1984).
[4] V. Zykov, *Simulation of Wave Processes in Excitable Media* (Manchester University Press, Manchester, 1987).
[5] Chaos **8** (1998), special issue on Fibrillation in normal ventricular myocardium, edited by A. T. Winfree.
[6] J. Morgan, D. Cunninggham, and E. Rowland, Br. Heart J. **67**, 42 (1992).
[7] P. Nánási, A. Varró, C. Pankucsi, P. Homolay, T. Knilans, L. Kovács, G. Papp, and D. Lathrop, Clin. Physiol. **16**, 339 (1996).
[8] M. Guevara, A. Ward, A. Shrier, and L. Glass, IEEE Comp. Cardiol. **562**, 167 (1984).
[9] M. Courtemanche, L. Glass, and J.P. Keener, Phys. Rev. Lett. **70**, 2182 (1993).
[10] A. Karma, Chaos **4**, 461 (1994).
[11] Z. Qu, J. Weiss, and A. Garfinkel, Am. J. Physiol. **276**, H269 (1999).
[12] A. Panfilov and A. Pertsov, Philos. Trans. R. Soc. London, Ser. A **359**, 1315 (2001).
[13] M. Franz, J. Schaefer, M. Schóttler, W. Seed, and M. Noble, Circ. Res. **53**, 815 (1983).
[14] J. Morgan, D. Cunninggham, and E. Rowland, J. Am. Coll. Cardiol. **19**, 1244 (1992).
[15] P. Szigligeti, T. Banyasz, J. Magyar, G. Szigeti, Z. Papp, A. Varro, and P. Nanasi, Acta Physiol. Scand. **163**, 139 (1998).
[16] K. Greenspan, R. Edmonds, and C. Fisch, Am. J. Physiol. **212**, 1416 (1967).
[17] J. Miller, A. Wallace, and M. Feezor, J. Mol. Cell. Cardiol. **2**, 3 (1971).
[18] M. Watanabe, N. Otani, and R. Guilmour, Circ. Res. **76**, 915 (1995).
[19] Z. Qu, J. Weiss, and A. Garfinkel, Phys. Rev. Lett. **78**, 1387 (1997).
[20] C. Zemlin and A. Panfilov, Phys. Rev. E **63**, 041912 (2001).
[21] F. Fenton, E. Cherry, H. Hastings, and S. Evans, Chaos **12**, 852 (2002).
[22] O. Bernus, R. Wilders, C. Zemlin, H. Verschelde, and A. Panfilov, Am. J. Physiol. **282**, H2296 (2002).
[23] B. Bass, Am. J. Physiol. **228**, 1717 (1975).
[24] A. Hodgkin and A. Huxley, J. Physiol. **117**, 500 (1952).
[25] W. H. Press, B. P. Flannery, S. A. Teukolsky, and W. T. Vetterling, *Numerical Recipes in C* (Cambridge University Press, Cambridge, NY, 1992).
[26] S. Rush and H. Larsen, IEEE Trans. Biomed. Eng. **25**, 389 (1978).
[27] F. Fenton and A. Karma, Chaos **8**, 20 (1998).
[28] A. Garfinkel, Y. Kim, O. Voroshilovsky, Z. Qu, J. Kil, M. Lee, H. Karagueuzian, J. Weiss, and P. Chen, Proc. Natl. Acad. Sci. U.S.A. **97**, 6061 (2000).
[29] O. Bernus, B. Van Eyck, H. Verschelde, and A. Panfilov, Phys. Med. Biol. **47**, 4167 (2002).
[30] Z. Qu, J. Weiss, and A. Garfinkel, Phys. Rev. E **61**, 727 (2000).
[31] M. Wellner, O. Berenfeld, and A. Pertsov, Phys. Rev. E **61**, 1845 (2000).
[32] A. Pertsov, M. Wellner, M. Vinson, and J. Jalife, Phys. Rev. Lett. **84**, 2738 (2000).
[33] M. Koller, M. Riccio, and R. Gilmour, Jr., Am. J. Physiol. **275**, H1635 (1998).